Microchim Acta
DOI 10.1007/s00604-016-1927-z

ORIGINAL PAPER

Ultrasound assisted dispersive micro solid-phase extraction of four tyrosine kinase inhibitors from serum and cerebrospinal fluid by using magnetic nanoparticles coated with nickel-doped silica as an adsorbent

Mehri Ghazaghi[1] · **Hassan Zavvar Mousavi**[1] · **Hamid Shirkhanloo**[2] · **Alimorad Rashidi**[3]

Received: 3 April 2016 / Accepted: 2 August 2016

Abstract Nanoparticles (NPs) consisting of a magnetic Fe_3O_4 core and a nickel(II)-doped silica shell were prepared and are shown to be viable materials for selective magnetic extraction of trace quantities of the tyrosine kinase inhibitors (TKIs) imatinib, nilotinib, erlotinib and sunitinib. The NPs were characterized by scanning electron microscopy, transmission electron microscopy, DLS and XRD analysis, and the results revealed a uniform in size (with a typical diameter of 40 nm) and a core-shell structure. The magnetic nanoadsorbent displays good affinity of the TKIs, probably because of the affinity between the Ni(II) ions of the NPs with the nitrogen atoms in the TKIs. The magnetism of the NPs enables them to be quickly separated from serum and cerebrospinal fluid samples. Imidazole, with its higher affinity for Ni(II) than that of the TKIs, was used for desorption of the TKIs from the NPs prior to their quantification by HPLC with UV detection. The detection limits are as low as 200, 480, 130, and 250 $ng \cdot L^{-1}$ for imatinib, sunitinib, erlotinib, and nilotinib, respectively. The intra-day precisions (RSDs) were lower than 4.0 %. The method displays a wide linear range. It was applied to the determination of TKIs in (spiked) human serum and cerebrospinal fluid and gave recoveries in the range from 94.6 to 98.6 %.

Keywords Imatinib · Sunitinib · Erlotinib · Nilotinib · Chronic myeloid leukemia · Tumor drugs · Nickel doped silica · Fe_3O_4@SiO_2 · Core-shell nanoparticles

Introduction

Tyrosine kinase inhibitors (TKIs), small drug molecules, block the intracellular signals that are driving signals for proliferation in many malignant cells [1]. Imatinib, nilotinib, erlotinib and sunitinib, some selective TKIs, have been developed for treatment of chronic myeloid leukaemia (CML), gastrointestinal stromal tumours (GIST), advanced renal cell carcinoma, primary brain tumours and non-small cell lung cancer [2, 3]. The relation between treatment consequence and plasma or cerebrospinal fluid (CSF) concentrations of several TKIs have been confirmed [4]. Although these drugs have high molecular activity and pharmacodynamics characteristics but their pharmacokinetic characteristics seem relatively less interesting. Most of these molecules are metabolized by enzymes and generate inactive metabolites [5], on the other hand, TKIs are bound extensively to plasma and tissue proteins (> 95 %) and only a small fraction is free to enter the cells to perform its pharmacological action [6]. In addition, conducted research reveal that trace amount of TKIs can penetrate through the blood brain barrier into the central nervous system (CNS), so that CSF TKIs concentrations were <1 % of their plasma concentrations [7]. Therefore, determination of low concentration of free TKIs in plasma and CSF, which is in connection with the pharmacological effect of a drug in the body, is an essential tool for the control of cancer,

Electronic supplementary material The online version of this article (doi:10.1007/s00604-016-1927-z) contains supplementary material, which is available to authorized users.

✉ Hassan Zavvar Mousavi
hzmousavi@semnan.ac.ir

[1] Department of Chemistry, College of Science, Semnan University, P.O. Box: 35131-19111, Semnan, Iran

[2] Occupational and Environmental Health Research Center (OEHRC), Iranian Petroleum Industry Health Research Institute (IPIHRI), P.O. Box: 1485733111, Tehran, Iran

[3] Nanotechnology Research Center, Research Institute of Petroleum Industry (RIPI), P.O. Box: 1485733111, Tehran, Iran

Published online: 10 August 2016

investigation of treatment efficacy, and severe drug-related adverse events [8].

Using bioanalytical assays for quantification TKIs are based on high-performance liquid chromatography–tandem mass spectrometric (LC/MS–MS) and high-performance liquid chromatography-UV method [9, 10]. Most of these methods have been developed to measure total TKIs in plasma, so preconcentration step is not required. But, in order to determine free TKIs in plasma, small fraction of drugs, a sensitive and accurate preconcentration procedure is essential as sample purification and concentration prior to HPLC analysis.

Recent trends in analytical chemistry are toward miniaturizing sample preparation techniques, because these developing microextraction methods overcome traditional method problems by reducing the amount of the organic solvent and performing extraction, preconcentration and sample clean-up in one step [11]. Some of these new extraction techniques such as solid phase extraction (SPE), liquid phase microextraction (LPME), solid phase microextraction (SPME) and dispersive liquid–liquid microextraction (DLLME) have been developed and have garnered much attention [11, 12]. Among them, SPE is a popular method due to its simplicity, rapidity, low cost, and needing low amounts of reagents [13]. Different adsorbents with wide chemical and physical properties can be used in SPE method and this is the key of success of this technique. Micro-solid-phase extraction (μ-SPE) and dispersive micro-solid-phase extraction (DμSPE), miniaturized formats of SPE, have been recently attracting attentions as they further reduce both solvent and sorbent consumption and facilitate sample handling [14, 15]. In the DμSPE mode sorbent completely is mixed with the sample solution by means of ultrasounds, vortex, sonication, or using an emulsifier, so allows high extraction efficiency due to increase interaction between sorbent and analytes.

Nanotechnology introduces different nanomaterials as a nanoadsorbent in different mode of SPE and creates specific properties for sample preparation methods such as large surface areas to volume ratio, rapid extraction kinetics, high extraction efficiencies, and reduction of sample amounts as well as toxic organic solvents [16]. Among the different nanomaterials, magnetic nanoparticles are the most popular because of simplifying sample preparation and overcoming some limitations of conventional SPE [17, 18]. Among the variety of nano-magnetic materials, magnetite (Fe_3O_4) has been the ones most extensively applied due to its good biocompatibility, particular physical and chemical properties and high potential of applications, not only in dispersive SPE but also in others such as cell separation, magnetically assisted drug delivery, enzyme immobilization [19, 20]. Magnetic nanoparticles (m-NPs) are usually modified and coated with different materials, inorganic (silica, etc.) and organic (surfactants, etc.) covers, in order to increase their stability and avoid agglomeration [21, 22]. The m-NPs tend to be oxidize so lead to loss of dispersability and magnetism [23, 24]. Besides that, surface modification increases extraction capacity and selectivity, so specific coatings not only overcome some limitations but also make further functionalization for successful interactions with the targets analytes.

In the present work, silicate as low cost, chemically stable, and biocompatible material was used for coating the surface of nano Fe_3O_4, then with adding nickel into structure of nanoadsorbent, it was converted to selective nanoadsorbent for extraction of four TKIs from complex matrices. The nanoadsorbent possesses high Ni^{2+} density on the surface and is easily separated magnetically. It was applied to selectively bind and separate TKIs from serum and cerebrospinal fluid sample. The Fe_3O_4@Ni_xSiO_y was applied in magnetic ultrasound assisted dispersive micro solid phase extraction (MUA-DμSPE) for preconcentration of four TKIs from human serum and CSF samples.

Experimental

Reagents and materials

Analytical grade of imatinib mesilate, nilotinib, erlotinib and sunitinib maleate were provided friendly by Parsian Pharmaceuticals Company (Tehran, Iran, parsian-pharma.co). HPLC grade acetonitrile, methanol and water were purchased from Ameretat Shimi (Tehran, Iran, http://www.ameretatco.com). Ammonia, $FeCl_3{\cdot}6H_2O$, $NaAc{\cdot}3H_2O$, Ethylene glycol, Polyethylene glycol (PEG, 6000), sodium dodecyl sulfate (SDS), and imidazole were prepared from Merck (Darmstadt, Germany; http://www.merckgroup.com). Tetraethyl orthosilicate (TEOS 98 %), nickel (II) chloride ($NiCl_2.6H_2O$), and ethanol were purchased from Sigma-Aldrich Chemie GmbH (Steinheim, Germany, www.sigmaaldrich.com/germany.html). The stock solutions of four TKIs were prepared by dissolving appropriate amount of them in HPLC-grade methanol at 1000 mg L^{-1} and stored in the dark at 4 °C. The working standard solutions were prepared daily by dilution of their stock standard solutions with HPLC-grade water. Drug-free (blank) human serum and cerebrospinal fluid samples from healthy donors were obtained from Baqiyatallah Hospital (Tehran, Iran, http://www.baq.ir/en).

Instrumental and analytical conditions

Separation and determination of four mentioned TKIs was performed using a Knauer HPLC system (Berlin, Germany) equipped with a K-1001 HPLC pump, D-14,163 online degasser, K-1500 solvent organizer, and a K-2600 UV detector. Chromatographic separation was performed at ambient temperature on Inertsill ODS-3 5 μm column 250 mm × 4.6 mm

(GL Science; Tokyo, Japan, www.glsciences.com), protected by a Guard column with Inertsustian C18 (4.0 mm × 3.0 mm) cartridge (GL Science; Tokyo, Japan). The pH solution was measured by a PHS-3BW model pH-meter (Bell, Italy) and dispersion of magnetic nano adsorbent was performed with the aid of ultrasonic waves by 50/60 KHz ultrasonic water bath (SW3, Switzerland). The synthesized nano material was characterized by transmission electron microscopy (TEM) Zeiss-EM10C - 80 KV and scanning electron microscopes (FESEM Sigma, Zeiss, Germany). The element composition of the synthesized material was characterized by an energy dispersive spectrometer (EDS) attached to the Zeiss FESEM. The X-ray diffraction (XRD) of samples was measured with a Philips PW1840 X-ray diffractometer (U.S. A) using Co-Ka radiation (λ = 1.78896 A), (40 kV and 25 mA conditions). UV-Vis spectra were obtained on a Shimadzu UV-1650 PC double-beam spectrophotometer. Size distribution and colloidal stability data were provided by VASCO nanoparticle size analyser based on the Dynamic Light Scattering (DLS, Corduan technologies, France). Zeta potentials of the prepared nanoparticles were measured by Particle Size Analyser (Dynamic laser light scattering, ZetaPlus, Brookhaven Instrument Co., USA).

Chromatography conditions

The optimum elution for separation of four mentioned TKIs on the analytical column was attained with a composition mobile phase of 20 mmol L^{-1} ammonium acetate (pH = 3.45) (A) and acetonitrile (B) with using gradient elution at a flow rate of 1.0 mL min^{-1}. The gradient elution program was as follows: at the time of injection (time of zero) the composition of the mobile phase was 95 % A and 5 % B, and during 11-min run the percentage of acetonitrile was gradually increased to 95 % and the percentage of buffer gradually decrease to 5 %. Then this percentage was kept constant for 5 min. Finally, the composition was changed back to 95 % A and 5 % B within 5 min and allow the chromatographic system was equilibrated for 5 min before the next injection. The injection volume was 20 μL and TKIs were monitored at 262 nm.

Sample preparation

Preparation of serum samples before MUA-DμSPE method in order to determine total TKIs (bonded and free) was based on protein precipitation with aid of acetonitrile. In this regard, appropriate volume of four mentioned TKI standard solution was spiked to 1.5 mL serum sample and shaken for 15 min, then 2.5 mL acetonitrile was added to the sample and vortex for 30 s. Then, this mixture was centrifuged for 15 min at 6000 rpm (2012 rcf) at room temperature and the supernatant was transferred into a glass tube and evaporated to dryness at 40 °C under nitrogen stream. The residual was dissolved in 1.5 mL deionized water and MUA-DμSPE method was done on the final solution.

In order to determine free TKIs in the serum sample, appropriate amount of TKI standard solution was added and shaken for 20 min for allowing to bind to proteins [25]. Then serum sample was placed in centrifuge filter tube and centrifuged for 10 min at 6000 rpm (corresponding to a rcf of 2012). Bonded TKIs remained in upper part and free TKIs was passed thought the filter and collected in lower part, so the serum sample collected in lower part was extracted by the MUA-DμSPE method.

Cerebrospinal fluid was applied without protein precipitation.

Synthesis of $Fe_3O_4@Ni_xSiO_y$ NPs

First, uniform magnetic cores were obtained via a solvothermal synthetic method, in which PEG and SDS were used as the protective agents to prevent the particles from aggregation. The solvothermal approach was selected due to the ability of this method to control particle size [26]. The synthetic procedure is as follows: $FeCl_3{\cdot}6H_2O$ (3.0 mmol), $NaAc{\cdot}3H_2O$ (15.0 mmol), and SDS (4.0 mmol) and PEG (0.4 g, ~7 mmol of the repeating units) were added to ethylene glycol (24.0 ml) to form colloid mixture under vigorous stirring at room temperature. Then, the mixture was transferred into a Teflon-lined stainless-steel autoclave of 50 ml capacity and sealed. Finally, the autoclave was heated and maintained at 180 °C for 24 h. After naturally cool down to room temperature, the back products were washed several times with absolute ethanol and dried at 60 °C for 6 h.

In second step, the magnetic cores were coated with a thin silica layer to obtain $Fe_3O_4@SiO_2$ NPs via a sol–gel approach [27]. In usual way, 0.20 g of Fe_3O_4 nanoparticles were dispersed by ultrasonication in 70 mL of mixed solution of ethanol–water–ammonia (50:20:1) and stirred with the help of mechanical agitation. Next, a mixture of TEOS (2 mL) and ethanol (30 mL) was added dropwise into the above solution. Following that the mixture was heated at 50 °C for 5 h to get $Fe_3O_4@SiO_2$ NPs. Then, the product was washed several times with water and absolute ethanol and dried at 60 °C for 3 h.

In third step, Ni ions were inserted into SiO_2 shell at an ammonia solution to form $Fe_3O_4@Ni_xSiO_y$ NPs. This step was done as follows: 0.10 g of $Fe_3O_4@SiO_2$ NPs were mixed by 10 mL of Ni^{2+} solution, containing 2 mmol $NiCl_2.6H_2O$ and 2.5 mL of NH_3. H2O, and transferred into a Teflon-lined stainless-steel autoclave and heated at 110 °C for 12 h. Afterward, the $Fe_3O_4@Ni_xSiO_y$ were obtained via an assistant magnet.

Ultrasound assisted dispersive micro solid phase extraction

The MUA-DμSPE procedure was performed as follows: 1.5 mL sample containing 40 μg L^{-1} four mentioned TKIs,

after adjusting sample pH .0 by adding nitric acid and sodium hydroxide solution, was placed in microtube (Eppendorf). Then, 2 mg Fe_3O_4@Ni_xSiO_y NPs was introduced into the mixture and immersed in ultrasonic water bath for 60 s in order to disperse the magnetic nanoadsorbent in throughout the sample solution effectively. Thereafter, separation of extracting phase was occurred with the aid of external magnet. The upper aqueous phase was removed with a syringe, the residue was eluted with 150 μL of THF containing 10×10^{-3} mol L^{-1} imidazole. After adding desorption solution, the mixture was placed in ultrasonic bath for 30 s and separated by the external magnet, therefore solution containing desorbed analytes was transferred into the clean tube and dried under nitrogen stream. The residue was redissolved in 40 μL of acetonitrile and injected into the HPLC system for separation and determination.

Results and discussion

Choice of materials

Magnetic separation as a rapid and efficient method for separation from aqueous systems has attracted much attention in analytical chemistry. So, Fe_3O_4 nanoparticles with high surface area and magnetic properties are a good selection. Fe_3O_4 NPs should be coated to avoid oxidation and agglomeration and also increase stability, in this goal silica as a biocompatible material was used to coat the magnetic NPs. Fe_3O_4@SiO_2 can interact with wide range of analytes in suitable pH, but for selective interaction, prepared Fe_3O_4@SiO_2 NPs should be modified with appropriate function. Investigating TKIs have much functional group in their structures that can play as ligand and bind with metal ions. On the other hand, metal silicate nanomaterials are good candidates due to stability in various chemical and physical environments, and they are widely used in adsorption, separation, and catalytic fields [28, 29]. Among different metal ions, nickel and cobalt play important role in biological system and have attracted significant interest in separation and bioanalytical approaches, such as separation of proteins and etc. [30, 31]. Imidazole was used for releasing bonded drugs and stability constant of Ni-imidazole is higher that Co-imidazole [32]. Accordingly, nickel was selected to modified silicate for selective interaction with TKIs.

Characterization of the Fe_3O_4@Ni_xSiO_y NPs

The morphologies and structure of Fe_3O_4@Ni_xSiO_y NPs were characterized by SEM, TEM, XRD and DLS analysis. Figure 1 indicates The XRD analysis of synthesized nanoparticles. The Fe_3O_4@Ni_xSiO_y exhibits multiple diffraction peaks, which are related to Fe_3O_4, $NiSiO_3$, and nickel hydroxide. Each of the diffraction peaks are indicated in Fig. 1 and confirmed presence the $NiSiO_3$ phase in the synthesized nanoparticles. These results approve that the Fe_3O_4 core was coated with nickel silicate shell. Moreover, the peaks correspond nickel hydroxide indicates that partial Ni ions exist in the form of nickel hydroxide.

Figure 2 indicates FESEM image of prepared Fe_3O_4@Ni_xSiO_y NPs. The FESEM image confirms that the synthesized nanoparticles are spherical in shape and the particles size is almost uniformly. The EDS analysis demonstrates (Fig. S1) the existence of nickel (Ni), iron (Fe), silicon (Si) and oxygen (O) in structure of synthesized magnetic nanoparticles and corroborates presence of Ni in shell structure.

TEM images of synthesized NPs present in Fig. 3, the core-shell structure of Fe_3O_4@Ni_xSiO_y can be clearly distinguished. As can be seen, the Fe_3O_4 cores are surrounded by a dense layer of nickel silicate shell with the thickness of 10 nm (the Fe_3O_4 core is black, while the nickel silicate shell is grey).

The size and size distribution of the Fe_3O_4@Ni_xSiO_y NPs in water were determined by DLS. Fig. S2 presents size distribution of the prepared nanoparticles, DLS analysis hydrodynamic size of the Fe_3O_4@Ni_xSiO_y NPs calculated as 40.78 nm that confirm obtained results by TEM. Size distribution measurements demonstrate narrow distribution range for synthesized nanoparticles. The surface charge was measured as zeta potential for each nanoparticle after each modification step and the results indicate in Fig. S3. These results show changes after each step, especially after modification with Ni^{2+}. The colloidal stability and/or aggregation test of the Fe_3O_4@Ni_xSiO_y NPs was evaluated as a function of intensity of scattered light and time in water media at pH and 25 °C, and result presents in Fig. S4. Reduction in the intensity of scattered light with time express instability and aggregation of the NPs in aqueous solution. This causes sedimentation of the NPs.

UV-vis absorption spectra of the four TKIs and their complexes with Ni^{2+} in methanol are displayed in Fig. S5. As can be seen, absorption spectra demonstrate complexation between Ni^{2+} and four TKIs. Peaks correspond to $n \rightarrow \pi^*$ disappear or peak intensity decrease from the UV-Vis spectra of the complexes, due to coordination of the ligand through non-bonding electrons. Also, for some complexes maximum peaks correspond to $\pi \rightarrow \pi^*$ shift to shorter wavelength (blue shift), may be due to the weakening of the π conjugation after coordination through the nitrogen atoms [33, 34]. Jobs method was applied to calculate stability constants of nickel complexes with the four TKIs and results were presented in Table S1. Stability constants for TKIs were lower than imidazole, it can interpret by basicity of the ligands (TKIs and imidazole). Imidazole in comparing with four TKIs is stronger base, so has more affinity toward Ni^{2+} and can form more stable complex. In addition, despite NH_3 basicity, it has lower affinity to make complex with Ni^{2+} in comparing with imidazole [32]. Higher stability constant of imidazole may be due to its ability to π-type interactions between imidazole and

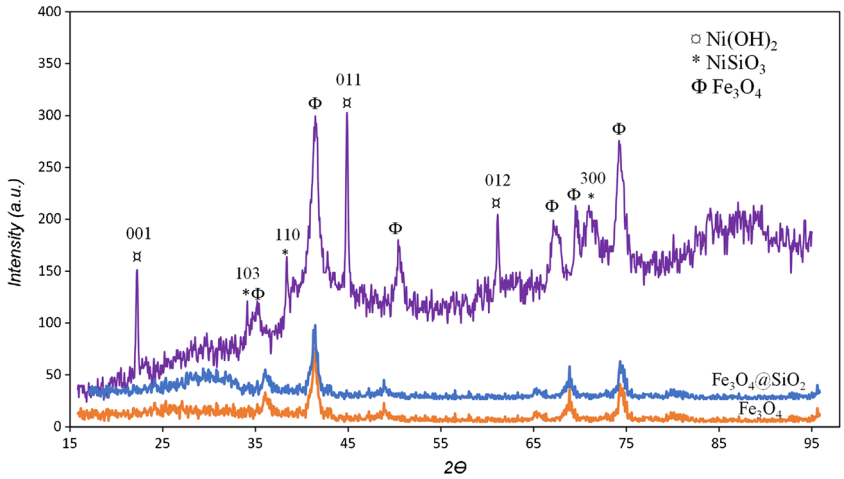

Fig. 1 XRD pattern of the $Fe_3O_4@Ni_xSiO_y$ NPs

nickel, that NH_3 is disable. Moreover, in this presented method desorption solvent was injected to RP-HPLC directly, high concentration of NH_3 destroy column.

Optimization of the ultrasound assisted dispersive micro solid phase extraction conditions

$Fe_3O_4@Ni_xSiO_y$ NPs were used in unprecedented procedure for selective interaction with four TKIs in human serum and CSF samples. Characterization analysis showed that synthesized magnetic NPs have Ni^{2+} ions in their surface, and it is an obvious fact that Ni is an electrophile ion. On the other hand, TKIs have amine group in their structure and act as a nucleophile. So, Ni^{2+} ions in surface of the NPs have high affinity toward the mentioned TKIs. It is obvious that Ni^{2+} complex on SiO_2 are weaker than complexation of the analytes to the free Ni^{2+} in solution and it can be considered as an advantage in eluting step. Prepared $Fe_3O_4@Ni_xSiO_y$ NPs were used in MUA-DμSPE procedure for selective extraction of four TKIs. Effecting parameters, including (a) sample pH, (b) adsorbent dosage, (c) extraction time and (d) desorption condition were investigated. Effect of sample pH is given in the main text.

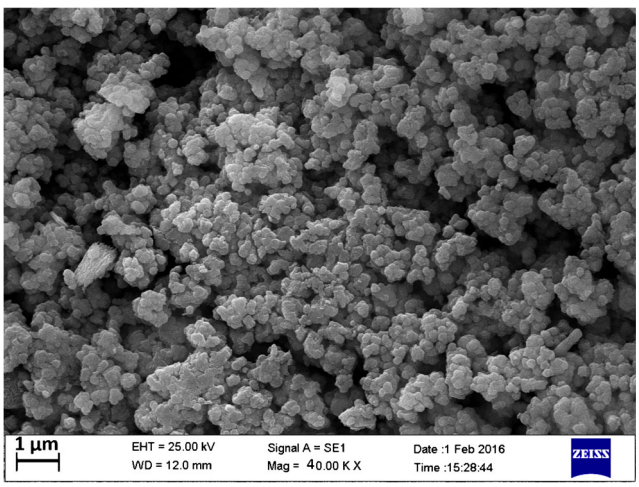

Fig. 2 SEM images of the $Fe_3O_4@Ni_xSiO_y$ NPs

Effect of sample pH

Since the MUA-DμSPE method is based on complexation of the mentioned TKIs with Ni^{2+} ions on surface of the $Fe_3O_4@SiO_2$ NPs, so pH is a critical parameter for bonding. In this regard, the influence of this parameter on the recovery of Imatinib, Sunitinib, Erlotinib and Nilotinib was investigated in the pH range of 2–10. The pH value was adjusted by adding adequate amounts of either HNO_3 or NaOH solutions. The results presented in Fig. 4 indicated that maximum recoveries were achieved in the pH range of 9–10. In acidic pH, nickel hydroxide bonded on surface of the NPs convert to Ni^{2+} with positive charge, and also, TKIs are positively charged due to protonation reaction of amine group in their structure. Therefore, as a result of repulsive force extraction recovery of the mentioned TKIs are low in acidic region. In basic pH, Ni ions on surface of the NPs are in form of the hydroxide and the TKIs molecules are in natural forms, so nucleophilic nitrogen atoms of the TKIs, with high affinity attack electrophilic Ni atoms, therefore complexes are formed. In this case, the TKIs can be extracted selectively. The pK_a values of Imatinib, Sunitinib, Erlotinib and Nilotinib (8.07, 8.95, 5.42 and 13.47, respectively) confirm these results. As a result, pH was selected in the subsequent process as the optimum pH.

In order to investigate necessity and role of Ni in the structure of prepared NPs, $Fe_3O_4@$ SiO_2 was prepared as a control and applied in presented procedure in the pH range of 2–10 and result indicated in Fig. S6. These results demonstrated that $Fe_3O_4@$ SiO_2 cannot extract TKIs effectively. Although silica at pH 2 is negatively charged and TKIs are organic compound with positively charged nitrogen groups, but these large

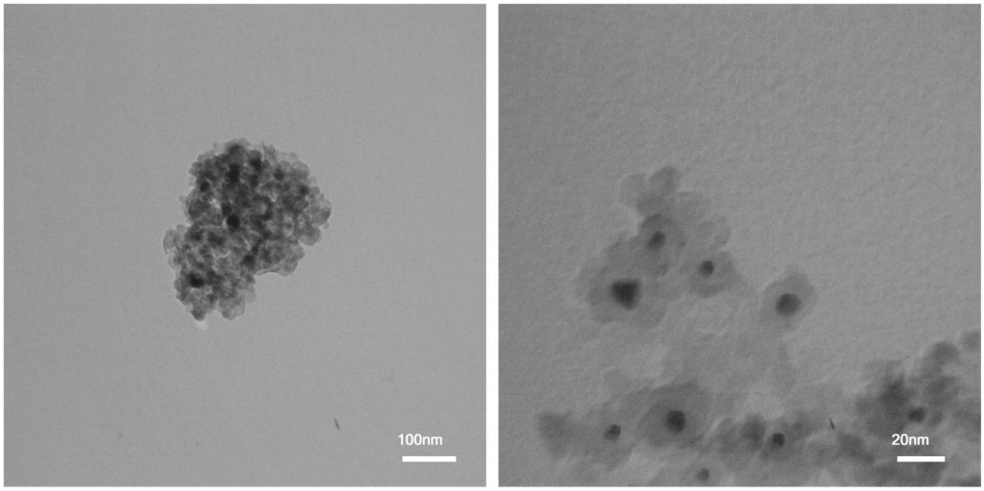

Fig. 3 TEM images of the $Fe_3O_4@Ni_xSiO_y$ NPs

organic structure of the TKIs have low tendency to adsorb electrostatically on polar surface of the silica. Extraction recoveries at pH in the range of 4–6 were about 12 (± 1.2, $n = 3$) %-15 (± 1.4, n = 3) % and reached to 2 (± 0.2, n = 3) -3(± 0.3, n = 3) % at pH . So, at pH , optimized pH for selective extraction by $Fe_3O_4@Ni_xSiO_y$, the TKIs were extracted just by interaction with Ni on the surface of the NPs. These results not only confirmed necessity and role of Ni in the structure of the prepared NPs for selective extraction of the TKIs, but also indicated affinity of TKIs toward Ni ions.

Others respective data and figures are given in the Electronic Supporting Material. The following experimental conditions were found to give best results: (a) sample pH value of 9; (b) 2 mg $Fe_3O_4@Ni_xSiO_y$ NPs; (c) 150 μL of THF containing 10 mmol L^{-1} imidazole; (d) extraction time of 1 min.

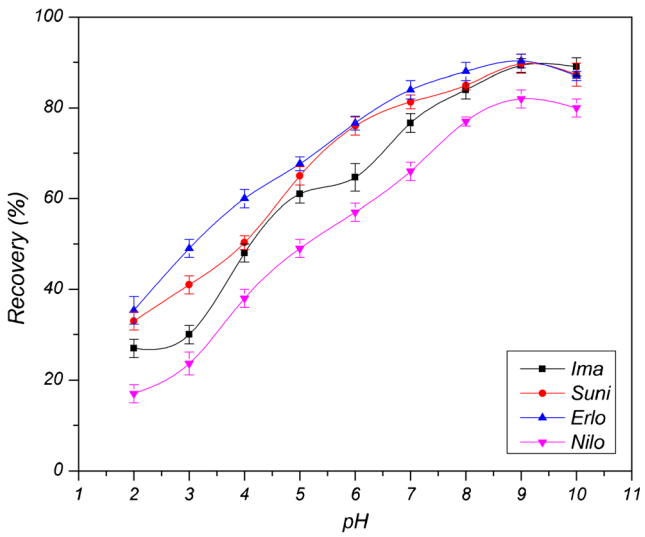

Fig. 4 Effect of sample pH on extraction recovery. Conditions: 1.5 mL sample solution containing 40 μg L^{-1} of each TKIs, 2 mg the $Fe_3O_4@Ni_xSiO_y$ NPs, 150 μL THF containing 10 mmol L^{-1} imidazole as a desorption solvent, extraction time: 1 min. (Mean of three determinations ± standard deviation)

Interference study

The presented method was based on complexation of the four TKIs with Ni^{2+}, so it was essential to investigate effect of common anions and EDTA on extraction of the TKIs. The interference of common anions and EDTA on the recovery of imatinib, sunitinib, erlotinib and nilotinib by the MUA-DμSPE method was investigated in the optimized procedure. The tolerance limit was defined as the amount of foreign ion, causing a change of less than ±5 % in the peak area. The results in Table S2 indicated that no significant variation in the absorbance was observed, it may due to presence of nickel in form of hydroxide and inability of these anions to compete with hydroxide anion. But, results for EDTA were different and this ligand interfered with extraction of these four TKIs. In presence of EDTA even in concentration ratio of 1, the TKIs did not extract quantitatively. It is predictable that some drugs may interfere with TKIs and extraction recoveries may be decreased in presence of drugs with functional groups in biological samples. But this situation is not very likely.

Stability of synthesized $Fe_3O_4@Ni_xSiO_y$

Extraction procedure was performed in basic condition. Due to examine stability of the synthesized $Fe_3O_4@Ni_xSiO_y$, the NPs was ultrasounicated in solution pH for 1 min then the NPs analysed with EDX. Presented result in Fig. S11 confirmed that the prepared NPs are resistant in basic solution, it may due to preparation in strong basic solution, presence of Ni in its structure, or low extraction time.

Comparison $Fe_3O_4@Ni_xSiO_y$ with $Fe_3O_4@SiO_2$

In order to demonstrate performance of the prepared adsorbent, the presented method was performed at optimized condition by $Fe_3O_4@SiO_2$ and extraction recoveries were compared. The obtained extraction efficiencies by $Fe_3O_4@SiO_2$

Table 1 Analytical performance of the TC-IL-MDμLSPE technique

Parameter	Imatinib	Sunitinib	Erlotinib	Nilotinib
Enrichment factor	199	118	448	126
Consumptive index (mL)	0.007	0.012	0.003	0.012
Detection limit in aqueous solution (3 s, μg L^{-1}; n = 10)	0.20	0.48	0.13	0.25
Detection limit in biological sample (3 s, μg L^{-1}; n = 10)	0.41	0.57	0.29	0.38
Intra-day precision (RSD %, n = 10)	3.4 (20 μg L^{-1})	3.8 (20 μg L^{-1})	3.5 (20 μg L^{-1})	4.0 (20 μg L^{-1})
Inter-day precision (RSD %, n = 5)	5.9 (20 μg L^{-1})	6.5 (20 μg L^{-1})	6.1 (20 μg L^{-1})	6.8 (20 μg L^{-1})
Linear range (μg L^{-1})	0.85–130	1.9–220	0.5–140	0.9–230
Correlation coefficient	0.9990	0.9981	0.9983	0.9987

for three replicated extractions were as follows: 7.3 ± 0.4, 4.7 ± 0.2, 8.4 ± 0.5 and 5.8 ± 0.3 for imatinib, sunitinib, erlotinib and nilotinib respectively. These results revealed that the Fe_3O_4@SiO_2 could not extract the four TKIs at pH , and further confirmed efficiency of the prepared Fe_3O_4@Ni_xSiO_y in extraction of the four TKIs.

Method evaluation

Under obtained optimum conditions, important parameters such as linear dynamic ranges (LDRs), precisions, limit of detections (LODs) and preconcentration factors (PFs) were determined to evaluate the method performance. High-quality linear relationships were gained in the extensive concentration range of 0.85–130 μg L^{-1} for imatinib, 1.9–220 μg L^{-1} for sunitinib, 0.5–140 μg L^{-1} for erlotinib and 0.9–230 μg L^{-1} for nilotinib with good correlation coefficients higher than 0.9981. Limits of detection were considered as standard deviation of blank signal intensity for 10 runs divided by the slope of the calibration curve, so LODs for imatinib, sunitinib, erlotinib and nilotinib were calculated as 0.20, 0.48, 0.13 and 0.25 μg L^{-1}, respectively. In order to investigate the repeatability of the presented method ten replicated extractions of four TKIs were performed at concentration of 50 μg L^{-1} by MUA-DμSPE method and intraday relative standard deviations (RSDs) were obtained 3.4, 3.8, 3.5 and 4.0 for imatinib, sunitinib, erlotinib and nilotinib, respectively. As well as, the reproducibility of the method, inter-day RSD of five replicates were measured and results indicated in Table 1. Characterization factors for preconcentration method such as enrichment factor (EF)

Table 2 Determination of free and whole TKIs in human serum and whole TKIs in cerebrospinal fluid samples by presented TC-IL-MDμLSPE method under optimum conditions. Method under optimum conditions

Sample	Added (μg L^{-1})				Found [a] (μg L^{-1})				Recovery (%)			
	Imatinib	Sunitinib	Erlotinib	Nilotinib	Imatinib	Sunitinib	Erlotinib	Nilotinib	Imatinib	Sunitinib	Erlotinib	Nilotinib
Human Serum	-	-	-	-	ND[b]	ND	ND	ND	-	-	-	-
	5.0	5.0	5.0	5.0	4.6 ± 1.9	4.7 ± 2.1	4.6 ± 2.0	4.5 ± 1.8	92.0	94.0	92.0	90.0
	50	100	50	100	47.3 ± 2.3	97.2 ± 3.5	47.8 ± 2.4	95.2 ± 3.8	94.6	97.2	95.6	95.2
	100	150	100	150	94.9 ± 4.1	146 ± 5.4	94.6 ± 4.1	142 ± 5.8	94.9	97.4	94.6	94.7
Human CSF	-	-	-	-	ND	ND	ND	ND	-	-	-	-
	5.0	5.0	5.0	5.0	4.8 ± 1.8	4.8 ± 2.0	4.7 ± 1.9	4.7 ± 1.7	96.0	96.0	94.0	94.0
	50	100	50	100	47.9 ± 2.6	98.0 ± 4.9	49.1 ± 3.5	97.6 ± 4.8	95.8	98.0	98.2	97.6
	100	150	100	150	97.8 ± 4.1	145 ± 5.6	97.2 ± 4.8	147 ± 5.4	97.8	96.7	97.2	98.0
Human Serum[c]					Found [a] (μg L^{-1})				Protein binding (%)			
					Free Imatinib	Free Sunitinib	Free Erlotinib	Free Nilotinib	Imatinib	Sunitinib	Erlotinib	Nilotinib
	50	100	50	100	1.7 ± 0.1	3.6 ± 0.3	1.5 ± 0.2	1.4 ± 0.1	96.6	96.4	97.0	98.6
	100	150	100	150	3.2 ± 0.2	4.1 ± 0.2	3.3 ± 0.3	2.5 ± 0.2	96.8	97.2	96.7	98.4

[a] Mean value ± standard deviation based on three replicate measurements

[b] Not detected

[c] prepared for determination of free TKIs

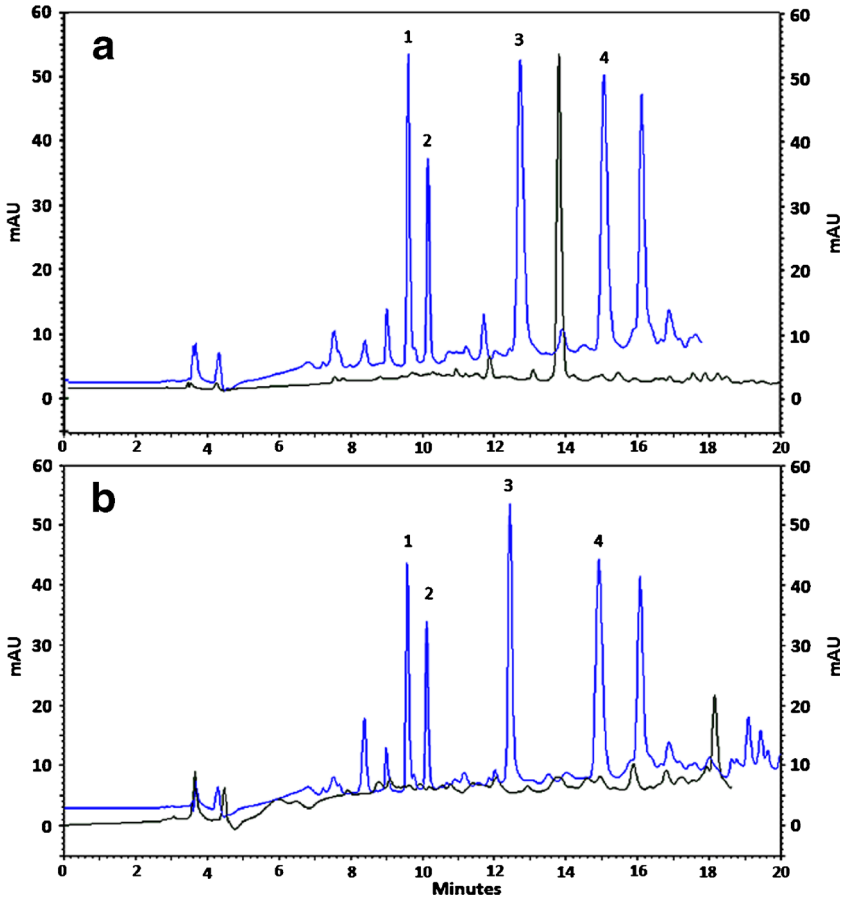

Fig. 5 Representative chromatograms under optimal TC-IL-MDμLSPE conditions. **a** Human CSF sample, green line: non-spiked CSF sample, *blue line*: spiked CSF sample at 60 μg L^{-1} of each TKIs. **b** Human serum sample, green line: non-spiked serum sample, *blue line*: spiked serum sample at 50 μg L^{-1} of each TKIs. (1) Imatinib, (2) Sunitinib, (3) Erlotinib, (4) Nilotinib

and consumptive index (CI) were also determined. Enrichment factor was calculated as the slope ratio of the calibration graph of the MUA-DμSPE procedure to that of the calibration graph without preconcentration and the consumptive index (CI) was defined as the sample volume (mL) consumed to reach a unit of enrichment factor (EF): CI = Vs (mL)/EF, where Vs is the sample volume. The analytical performances of the presented method are presented in Table 1.

Application of ultrasound assisted dispersive micro solid phase extraction method to serum and cerebrospinal fluid sample

In order to investigate matrix effect on the presented method, the MUA-DμSPE approach was applied to the simultaneous analysis of four TKIs in human serum and cerebrospinal fluid samples. Human real samples were spiked with the four TKI standard solution at different

Table 3 Comparison of the MUA-DμSPE procedure with published method for preconcentration and extraction of TKIs

TKIs	Method	Detection	Matrix	LOD (μg L^{-1})	RSD %	Calibration range (μg L^{-1})	PF/EF	Sample volume	Ref.
Imatinib, Sunitinib, Erlotinib, Nilotinib, Axitinib, Gefitinib, Dasatinib	solid-phase extraction	UPLC/ MS-MS	Plasma	0.1 dasatinib and axitinib 0.4 gefinitinib and sunitinib	13.1 and 14.2 %	0.1/0.4–200	30 [b]	5 mL	[35]
Imatinib, Sunitinib, Erlotinib, Nilotinib	MUA-DμSPE	HPLC-UV	Serum and CSF	0.20, 0.48, 0.13, 0.25	3.4, 3.8, 3.5 and 4.0 %	0.85–130, 1.9–220, 0.5–140, 0.9–230	119, 118, 448 and 126 [a] 37.5 [b]	1.5 mL	This study

[a] slopes ratio of calibration curves of analyte after preconcentration to that prior preconcentration (PF)

[b] volume ratio before and after preconcentration (EF)

concentrations in corresponding linear ranges. As previously mentioned, protein bounding of the TKIs are more than 95 %, so determination of free and total TKIs in serum samples were performed in separate sample preparation procedure presented in section of sample preparation, then the MUA-DμSPE method was applied (n = 3) for extraction and preconcentration of mentioned TKIs from serum samples. Whereas, just detection of the total TKIs were performed in CSF samples, so the MUA-DμSPE procedure was accomplished (n = 3) on CSF samples without sample preparation. So, the presented results in Table 2 were provided in two separate parts, in the first part of the table, experimental data for determination of total TKIs were presented and in the second part, free TKIs in serum sample were measured. Actually, method validation was performed by determination of total TKIs in spiked human serum and CSF samples and determination of free TKIs were performed not only in order to examine capability of the method in detection of negligible concentration of the drugs, but also results of binding percentage furthermore confirmed validation of the method. The recoveries of total drugs were in the acceptable range of 92.0 (±2, n = 3) – 98.6 (±4, n = 3) %, exhibited that the present method is effective for the determination of TKIs in complex matrices such as serum and CSF samples. Detecting results of free (no bonded to protein) TKIs in serum samples confirm reported values for protein bindings of the four TKIs. These results demonstrate capability of the MUA-DμSPE procedure in detection of the mentioned TKIs even in trace amount in complex matrices, and also the agreement between the obtained binding percentages and reported values furthermore confirmed the accuracy of the method. The typical chromatograms of non-spiked and spiked human serum and CSF with 60 and 50 μg L^{-1} of each TKIs are presented in Fig. 5. Also, the chromatogram of the four TKI standard solutions was presented in Fig. S12.

Comparison of the ultrasound assisted dispersive micro solid phase extraction method with existing extraction procedures

A comparison of the presented method with other reported methods in determination of imatinib, sunitinib, erlotinib and nilotinib can be found in Table 3. Unfortunately, there is just one reported method for extraction and preconcentration of the TKIs. As can be seen, the presented method possesses a wide range of linearity, low detection limit, high sensitivity, and low consumption of sample volume for simultaneous extraction of the TKIs. LODs of the MUA-DμSPE method were comparable with reported method only with use of 1.5 mL sample solution. Also, higher enrichment factors obtained with preconcentration of lower sample volume while having better precision indicate that the presented method is applicable and reliable for detection of the TKIs. Also in comparing with reported method, the MUA-DμSPE procedure is very fast and easy to do (extraction was performed in 1 min).

Most of the presented adsorbents for extraction of drugs were based of adsorption of analytes through hydrophobic interaction. So in biological samples and complex matrices, adsorbent interact with analytes along with macromolecule and other hydrophobic interferences. But prepared $Fe_3O_4@Ni_xSiO_y$ NPs can interact just with TKIs through complexation at appropriate pH in presence of macromolecules and other interference in complex matrices, without any interaction with macromolecules existing in samples. Because in optimized pH and condition just the four TKIs can bind to the $Fe_3O_4@Ni_xSiO_y$ NPs.

Conclusion

The $Fe_3O_4@Ni_xSiO_y$ NPs as a nanoadsorbent was successfully applied in easy operating magnetic ultrasound assisted dispersive micro solid phase extraction (MUA-DμSPE) method for selective extraction and preconcentration of imatinib, sunitinib, erlotinib and nilotinib in human serum and CSF samples. Magnetic $Fe_3O_4@SiO_2$ NPs were prepared by solvothermal approach and result of EDX analysis indicated that surface of the nanoparticles was modified with nickel ions for selective adsorption of four TKIs from complex matrices. Results of DLS and TEM analysis confirmed that size of synthesized were about 40 nm with appropriate distribution. UV-vis absorption spectra corroborated interaction and complexation of TKIs with Ni^{2+}. Collection of solid phase was performed easily with aid of external magnet. Very scant amount of $Fe_3O_4@Ni_xSiO_y$ NPs hybrid were exploited in the MUA-DμSPE procedure. The results have been proved that the presented MUA-DμSPE method has low extraction time, it may be due to the high surface area to volume of the synthesized nanoparticles. The MUA-DμSPE method exhibited satisfactory reproducibility and low limit of detection. Performance of The MUA-DμSPE method in complex matrices was investigated by applying to extract trace mentioned TKIs from human serum and CSF sample. The satisfactory recoveries indicated that the MUA-DμSPE procedure can be considered as an accurate, efficient, and sensitive technique even for biological investigations.

Acknowledgments The authors would like to express their appreciation to the Semnan University Research Council for financial support of this study. The authors also thank Dr. Moazeni (Tehran, Iran, parsian-pharma.co) for providing studied drugs.

Compliance with ethical standards The author(s) declare that they have no competing interests.

References

1. Steeghs N, Nortier JW, Gelderblom H (2007) Small molecule tyrosine kinase inhibitors in the treatment of solid tumors: an update of recent developments. Ann Surg Oncol 14(2):942–953
2. Motzer RJ, Michaelson MD, Redman BG, Hudes GR, Wilding G, Figlin RA, Ginsberg MS, Kim ST, Baum CM, DePrimo SE (2006) Activity of SU11248, a multitargeted inhibitor of vascular endothelial growth factor receptor and platelet-derived growth factor receptor, in patients with metastatic renal cell carcinoma. J Clin Oncol 24(1):16–24
3. Padmalatha M, Kulsum S, Rahul C, Thimma Reddy D, Vidyasagar G (2011) Spectrophotometric methods for the determination of erlotinib in pure and pharmaceutical dosage forms. Int J Pharm Res Dev 3(6):103–109
4. Larson RA, Druker BJ, Guilhot F, O'Brien SG, Riviere GJ, Krahnke T, Gathmann I, Wang Y (2008) Imatinib pharmacokinetics and its correlation with response and safety in chronic-phase chronic myeloid leukemia: a subanalysis of the IRIS study. Blood 111(8):4022–4028
5. Rudin CM, Liu W, Desai A, Karrison T, Jiang X, Janisch L, Das S, Ramirez J, Poonkuzhali B, Schuetz E (2008) Pharmacogenomic and pharmacokinetic determinants of erlotinib toxicity. J Clin Oncol 26(7):1119–1127
6. Blay J-Y (2009) Pharmacological management of gastrointestinal stromal tumours: an update on the role of sunitinib. Ann Oncol. doi:10.1093/annonc/mdp291
7. Neville K, Parise RA, Thompson P, Aleksic A, Egorin MJ, Balis FM, McGuffey L, McCully C, Berg SL, Blaney SM (2004) Plasma and cerebrospinal fluid pharmacokinetics of imatinib after administration to nonhuman primates. Clin Cancer Res 10(7):2525–2529
8. Baccarani M, Saglio G, Goldman J, Hochhaus A, Simonsson B, Appelbaum F, Apperley J, Cervantes F, Cortes J, Deininger M (2006) Evolving concepts in the management of chronic myeloid leukemia: recommendations from an expert panel on behalf of the European LeukemiaNet. Blood 108(6):1809–1820
9. Lankheet N, Hillebrand M, Rosing H, Schellens J, Beijnen J, Huitema A (2013) Method development and validation for the quantification of dasatinib, erlotinib, gefitinib, imatinib, lapatinib, nilotinib, sorafenib and sunitinib in human plasma by liquid chromatography coupled with tandem mass spectrometry. Biomed Chromatogr 27(4):466–476
10. Roth O, Spreux-Varoquaux O, Bouchet S, Rousselot P, Castaigne S, Rigaudeau S, Raggueneau V, Therond P, Devillier P, Molimard M (2010) Imatinib assay by HPLC with photodiode-array UV detection in plasma from patients with chronic myeloid leukemia: comparison with LC-MS/MS. Clin Chim Acta 411(3):140–146
11. Cavaliere B, Monteleone M, Naccarato A, Sindona G, Tagarelli A (2012) A solid-phase microextraction-gas chromatographic approach combined with triple quadrupole mass spectrometry for the assay of carbamate pesticides in water samples. J Chromatogr A 1257:149–157
12. Payán MR, López MÁB, Fernández-Torres R, Navarro MV, Mochón MC (2011) Hollow fiber-based liquid phase microextraction (HF-LPME) for a highly sensitive HPLC determination of sulfonamides and their main metabolites. J Chromatogr B 879(2):197–204
13. Fritz JS (1999) Analytical solid-phase extraction. Wiley-Vch
14. Basheer C, Narasimhan K, Yin M, Zhao C, Choolani M, Lee HK (2008) Application of micro-solid-phase extraction for the determination of persistent organic pollutants in tissue samples. J Chromatogr A 1186(1):358–364
15. Ramandi NF, Shemirani F, Farahani MD (2014) Dispersive solid phase extraction of lead (II) using a silica nanoparticle-based ionic liquid ferrofluid. Microchim Acta 181(15–16):1833–1841
16. Ríos A, Zougagh M, Bouri M (2013) Magnetic (nano) materials as an useful tool for sample preparation in analytical methods. A review Anal Method 5(18):4558–4573
17. Cui Y, Liu S, Wei K, Liu Y, Hu Z (2015) Magnetic solid-phase extraction of trace-level mercury (II) ions using magnetic core-shell nanoparticles modified with thiourea-derived chelating agents. Microchim Acta 182(7–8):1337–1344
18. Kamran S, Asadi M, Absalan G (2013) Adsorption of acidic, basic, and neutral proteins from aqueous samples using Fe3O4 magnetic nanoparticles modified with an ionic liquid. Microchim Acta 180(1–2):41–48
19. Martín M, González Orive A, Lorenzo-Luis P, Hernández Creus A, González-Mora JL, Salazar P (2014) Quinone-rich poly (dopamine) magnetic nanoparticles for biosensor applications. Chem Phys Chem 15(17):3742–3752
20. Safari M, Yamini Y, Tahmasebi E, Ebrahimpour B (2016) Magnetic nanoparticle assisted supramolecular solvent extraction of triazine herbicides prior to their determination by HPLC with UV detection. Microchim Acta 183(1):203–210
21. Giokas DL, Zhu Q, Pan Q, Chisvert A (2012) Cloud point–dispersive μ-solid phase extraction of hydrophobic organic compounds onto highly hydrophobic core–shell Fe 2 O 3@ C magnetic nanoparticles. J Chromatogr A 1251:33–39
22. Eskandari H, Naderi-Darehshori A (2012) Preparation of magnetite/poly (styrene-divinylbenzene) nanoparticles for selective enrichment-determination of fenitrothion in environmental and biological samples. Anal Chim Acta 743:137–144
23. Wang Y, Tian T, Wang L, Hu X (2013) Solid-phase preconcentration of cadmium (II) using amino-functionalized magnetic-core silica-shell nanoparticles, and its determination by hydride generation atomic fluorescence spectrometry. Microchim Acta 180(3–4):235–242
24. Zhai Y, He Q, Han Q (2012) Solid-phase extraction of trace metal ions with magnetic nanoparticles modified with 2, 6-diaminopyridine. Microchim Acta 178(3–4):405–412
25. Bolandnazar S, Divsalar A, Valizadeh H, Khodaei A, Zakeri-Milani P (2013) Development and application of an HPLC method for erlotinib protein binding studies. Analysis 19(21):22
26. Yan A, Liu X, Qiu G, Wu H, Yi R, Zhang N, Xu J (2008) Solvothermal synthesis and characterization of size-controlled Fe 3 O 4 nanoparticles. J Alloys Compd 458(1):487–491
27. Deng Y, Qi D, Deng C, Zhang X, Zhao D (2008) Superparamagnetic high-magnetization microspheres with an Fe3O4@ SiO2 core and perpendicularly aligned mesoporous SiO2 shell for removal of microcystins. J Am Chem Soc 130(1):28–29
28. Qu J, Li W, Cao C-Y, Yin X-J, Zhao L, Bai J, Qin Z, Song W-G (2012) Metal silicate nanotubes with nanostructured walls as superb adsorbents for uranyl ions and lead ions in water. J Mater Chem 22(33):17222–17226
29. Fang Q, Xuan S, Jiang W, Gong X (2011) Yolk-like micro/nanoparticles with Superparamagnetic iron oxide cores and hierarchical nickel silicate shells. Adv Funct Mater 21(10):1902–1909
30. Wegner SV, Spatz JP (2013) Cobalt (III) as a stable and inert mediator ion between NTA and His6-tagged proteins. Angew Chem Int Ed 52(29):7593–7596
31. Xie H-Y, Zhen R, Wang B, Feng Y-J, Chen P, Hao J (2010) Fe3O4/Au Core/Shell nanoparticles modified with Ni2 + − Nitrilotriacetic acid specific to histidine-tagged proteins. J Phys Chem C 114(11):4825–4830
32. Sundberg RJ, Martin RB (1974) Interactions of histidine and other imidazole derivatives with transition metal ions in chemical and biological systems. Chem Rev 74(4):471–517

33. Felicio R, Cavalheiro E, Dockal E (2001) Preparation, characterization and thermogravimetric studies of [N, N′-cis-1, 2-cyclohexylene bis (salicylideneaminato)] cobalt (II) and [N, N ′-(±)-trans-1, 2-cyclo-hexylene bis (salicylideneaminato)] cobalt (II. Polyhedron 20(3):261–268
34. Salehi M, Amirnasr M, Meghdadi S, Mereiter K, Bijanzadeh HR, Khaleghian A (2014) Synthesis, characterization, and X-ray crystal structure of cobalt (III) complexes with a N 2 O 2-donor Schiff base and ancillary ligands. Spectral, antibacterial activity, and electrochemical studies. Polyhedron 81:90–97
35. Bouchet S, Chauzit E, Ducint D, Castaing N, Canal-Raffin M, Moore N, Titier K, Molimard M (2011) Simultaneous determination of nine tyrosine kinase inhibitors by 96-well solid-phase extraction and ultra performance LC/MS-MS. Clin Chim Acta 412(11):1060–1067